Anion Rearrangements in Fluorinated $Nd_2CuO_{3.5}$

G. Corbel and J. P. Attfield

Department of Chemistry, University of Cambridge, Lensfield Road CB2 1EW Cambridge, U.K.

J. Hadermann

EMAT, University of Antwerp (RUCA), Groenenborgerlaan 171, B-2020 Antwerp, Belgium

A. M. Abakumov,* A. M. Alekseeva, M. G. Rozova, and E. V. Antipov

Department of Chemistry, Moscow State University, Moscow 119899, Russia

Received January 11, 2002. Revised Manuscript Received September 19, 2002

$Nd_2CuO_{3.5}$, a derivative of Nd_2CuO_4 with anion-deficient ($CuO_{1.5}\square_{0.5}$) layers, has been fluorinated with XeF_2 at temperatures between 100 and 400 °C. Samples fluorinated at 200−300 °C exhibit superconductivity with critical temperatures of 6−11 K. Electron microscopy investigations revealed a complicated microstructure in both the initial and fluorinated phases. $Nd_2CuO_{3.5}$ is characterized by the presence of numerous twins which are caused by the lowering of the symmetry after a topotactic oxygen removal from the parent Nd_2CuO_4 phase. Fluorination at 200 °C leads to an increase of the formal copper valence and to a restoration of the T′-type structure. It is suggested that fluorine replaces oxygen in the Nd_2O_2 slab and the released oxygen atoms migrate into the ($CuO_{1.5}\square_{0.5}$) layers thus forming conducting (CuO_2) planes. This rearrangement shows a close resemblance to that previously found in fluorinated A_2CuO_3 (A = Ca, Sr). Local areas of fluorinated phases with larger values of the *c* parameter were found in the matrix of T′ phase. At 300 °C the monoclinic $Nd_2Cu(O,F)_5$ phase is also formed ($a \approx 13.2$ Å, $b \approx 5.5$ Å, $c \approx 5.8$ Å, $\beta \approx 92°$, space group *C*2/*c*) with a chainlike ordering of the empty and filled anion positions in the $Nd_2(O,F)_3$ blocks and buckled (CuO_2) planes due to a tilt of the $Cu(O,F)_6$ octahedra.

Introduction

Ln_2CuO_4 oxides (Ln = lanthanide) adopt three different structures types: the K_2NiF_4-type structure (T) with octahedrally coordinated Cu^{2+}, the Nd_2CuO_4-type structure (T′) where copper ion resides in a square planar, and the T*-type structure with square-based pyramids CuO_5 as found in $(Nd,Ce,Sr)_2CuO_4$. In these materials, superconductivity can be induced by a change of the charge carrier concentration (hole or electron doping). It can be performed either by heterovalent cationic substitution ($Nd_{1.85}Ce_{0.15}CuO_4$,[1] $Pr_{1.85}Th_{0.15}CuO_4$,[2] or $La_{2-x}(Sr,Ba)_xCuO_4$[3,4]) or anionic insertion/substitution ($La_2CuO_{4+\delta}$,[5] $La_2Cu(O,F)_{4.18}$,[6] or $Nd_2CuO_{3.7}F_{0.3}$[7,8]).

Among the numerous complex copper-based oxyfluorides there are examples of fluorination in which there is not only a simple insertion of fluorine into vacant anion sites or a substitution of fluorine for oxygen, but which also involve a rearrangement of the oxygen and fluorine atoms in the structure followed in some cases by drastic changes in the properties. The A_2CuO_3 (A = Ca, Sr) compounds possess a structure which can be derived from that of K_2NiF_4 by removing oxygen atoms from the (CuO_2) planes in an ordered manner,[9] resulting in the chains of corner-shared CuO_4 squares, whereas the A_2O_2 rock salt slabs remain unchanged. Thus, the (CuO_2) planes, which are necessary for superconductivity, are absent in this structure. Fluorination with a subsequent reductive treatment allows the superconducting phase $Sr_2CuO_2F_{2+\delta}$ with a T_C of 46 K[10] to be obtained. As was proposed in reference 10, oxygen atoms migrate from the Sr_2O_2 block and complete the equatorial coordination of the Cu atoms, resulting in the appearance of (CuO_2) planes. The apical positions of the CuO_4F_2 octahedra are occupied by fluorine atoms. An increase of the copper oxidation state is achieved by the insertion of an extra amount of fluorine atoms into the tetrahedral interstices of the Sr_2F_2 block. In contrast to $Sr_2CuO_2F_{2+\delta}$, which has a T-type structure, the Ca-based compound adopts the structure of the T′ phase, in agreement with the smaller size of the Ca cation.

* Corresponding author. Fax: +7-095-939-4788. E-mail: abakumov@icr.chem.msu.ru.

(1) Tokura, T.; Takagi, H.; Uchida, S. *Nature* **1989**, *337*, 345.
(2) Markert, J. T.; Early, E. A.; Bjørnholm, T.; Ghamaty, S.; Lee, B. W.; Neumeier, J. J.; Price, R. D.; Seaman, C. L.; Maple, M. B. *Physica C* **1989**, *158*, 178.
(3) Cava, R. J.; van Dover, R. B.; Batlogg, B.; Rietman, E. A. *Phys. Rev. B* **1987**, *35*, 5337.
(4) Modenbaugh, A. R.; Xu, Y., Suenaga, M.; Folkerts, T. J.; Snelton, R. N. *Phys. Rev. B* **1988**, *38*, 4596.
(5) Schirber, E.; Morosin, B.; Merill, R. M.; Hlava, P. F.; Venturini, E. L.; Kurak, J. F.; Nigrey, P. J.; Baughman, R. J.; Ginley, D. S. *Physica C* **1988**, *152*, 121.
(6) Tissue, B. M.; Cirillo, K. M.; Wright, J. C.; Daeumling, M.; Larbalestier, D. C. *Solid State Commun.* **1988**, *65*, 51.
(7) James, A. C. W. P.; Zahurak, S. M.; Murphy, D. W. *Nature* **1989**, *338*, 240.
(8) Tighezza, A.; Rehspringer, J. L.; Drillon, M. *Physica C* **1992**, *198*, 209.
(9) Weller, M. T.; Lines, D. R. *J. Solid State Chem.* **1989**, *82*, 21.
(10) Al-Mamouri, M.; Edwards, P. P.; Greaves, C.; Slaski, M. *Nature* **1994**, *369*, 382.

10.1021/cm021102m CCC: $25.00
Published on Web 11/26/2002

Despite the reasonably short in-plane Cu−O distances suitable for p-type superconductivity (1.925 Å), $Ca_2CuO_2F_{2+\delta}$ does not exhibit superconductivity, probably due to an insufficient copper valence.[11]

$Nd_2CuO_{3.5}$ is an anion-deficient derivative of the T′ phase, consisting of fluorite-type Nd_2O_2 slabs and ($CuO_{1.5}\square_{0.5}$) layers with Cu atoms in dumbbell and strongly distorted square−planar coordinations.[12] One may expect that the fluorination of this compound would cause structure transformations similar to those observed for the A_2CuO_3 compounds derived from the T structure. The fluorination of $Nd_2CuO_{3.5}$ will enable the behavior of A_2O_2 blocks with rock salt and with fluorite type structures to be compared when undergoing anion rearrangements accompanied by a migration of oxygen atoms to vacant anion positions in the (CuO_{2-x}) layers. In this contribution we describe the anion rearrangement in fluorinated $Nd_2CuO_{3.5}$, followed by a formation of (CuO_2) planes and the appearance of superconducting properties.

Experimental Section

Polycrystalline Nd_2CuO_4 was prepared by solid-state reaction from a stoichiometric mixture of Nd_2O_3 and CuO at 1100 °C. To obtain the oxygen-defect-ordered $Nd_2CuO_{3.5}$, a low-temperature topotactic reduction of Nd_2CuO_4, in a H_2 flow at 290 °C for 1.5 h, is performed on a thin layer of powder spread evenly in an alumina boat.[12−13] An iodometric titration revealed the average oxidation state of copper to be equal to +1.0. The cell parameters of $Nd_2CuO_{3.5}$ (a = 12.660(9) Å, b = 3.7659(8) Å, c = 8.485(4) Å, β = 109.58(4)°) are in agreement with those previously published.[12] The fluorination was performed with XeF_2. A 0.4-g aliquot of $Nd_2CuO_{3.5}$ was mixed with an appropriate amount of XeF_2 (provided by the Laboratory of Inorganic Synthesis of the Institute of Applied Chemical Physics, Kurchatovskii Institut, Moscow, Russia) in an N_2-filled glovebox, placed into a Ni crucible, and then sealed into an N_2-filled copper tube. The samples were annealed at temperatures ranging from 100 to 400 °C for 15 h and then the furnace was cooled to room temperature.

The phase composition of the samples and the lattice parameters of the compounds were determined by X-ray diffraction using a focusing Guinier-camera FR-552 (Cu $K_{\alpha 1}$ radiation, germanium internal standard) and a STADI-P powder diffractometer (Cu $K_{\alpha 1}$ radiation, curved Ge monochromator, transmission mode, linear PSD). The formal copper valences were determined by iodometric titration with estimated standard deviation of ±0.04.

Magnetization measurements were carried out on a SQUID magnetometer (Quantum Design Magnetic Property Measurement System 2). Powdered samples were zero field cooled and the temperature dependence of the magnetization was recorded under an applied magnetic field of 3 G from 5 to 150 K.

Electron diffraction (ED) and high-resolution electron microscopy (HREM) were performed using a JEOL 4000EX instrument. EDX analysis together with electron diffraction were carried out using a Philips CM20 microscope with a LINK-2000 attachment. Image simulations were made using MacTempas software.

Results

1. Sample Characterization. X-ray diffraction study of fluorinated samples revealed that the treatments of

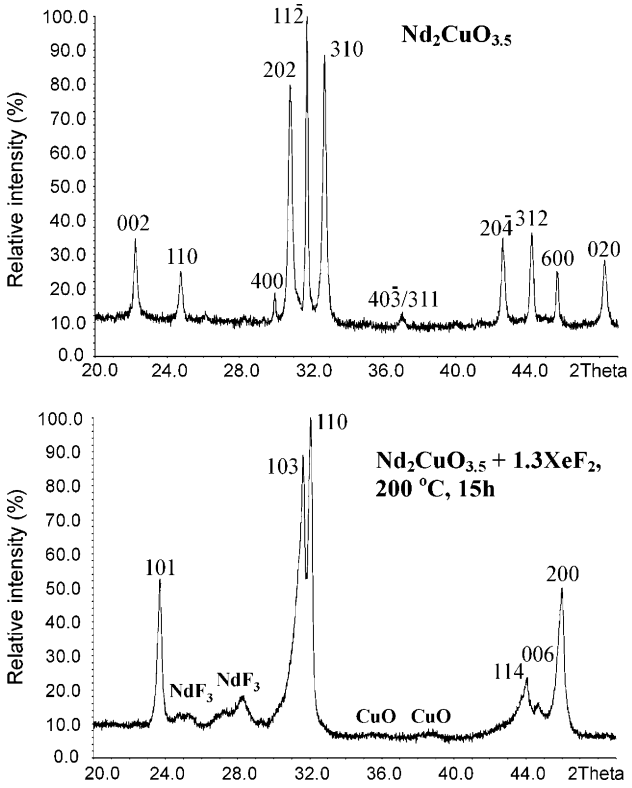

Figure 1. X-ray diffraction patterns of the initial $Nd_2CuO_{3.5}$ and after a fluorination at 200 °C with $Nd_2CuO_{3.5}/XeF_2$ = 1:1.3.

$Nd_2CuO_{3.5}$ with XeF_2 taken at 1:1−1:1.5 molar ratio at 100 °C does not significantly change the lattice parameters of the initial monoclinic phase. Therefore, we can conclude that at such temperature no noticeable amount of fluorine is inserted into the structure. However, the sample resulting after heating $Nd_2CuO_{3.5}$ at 100 °C with a very large excess of XeF_2 corresponding to a 1:5 molar ratio shows an increase of average copper oxidation state up to +1.28, whereas the lattice parameters of the phase under fluorination remain nearly unchanged: a = 12.649(6) Å, b = 3.7701(8) Å, c = 8.481(2) Å, β = 109.58(4)°. This may suggest a partial decomposition of the initial phase by large excess of XeF_2 with a formation of amorphous products containing Cu in oxidation states higher than +1. Increasing the temperature of the fluorination up to 200 °C results in a transformation of the monoclinic $Nd_2CuO_{3.5}$-type structure into the tetragonal Nd_2CuO_4 type structure. The X-ray diffraction pattern of the initial $Nd_2CuO_{3.5}$ phase and the sample obtained by a fluorination at 200 °C with $Nd_2CuO_{3.5}/XeF_2$ = 1:1.3 are shown in Figure 1. The main reflections in the X-ray diffraction pattern of the fluorinated phase can be indexed on the basis of a body-centered tetragonal unit cell with parameters a = 3.949(1) Å and c = 12.157(6) Å which are close to the cell parameters of Nd_2CuO_4 (a = 3.9423(2) Å, c = 12.1667(7) Å). Except for the reflections belonging to the T′-type phase, some very broad reflections are visible which can be attributed to a NdF_3 and CuO secondary phases. Thus, a fluorine insertion resulting in a transition from monoclinic $Nd_2CuO_{3.5}$ to tetragonal T′ fluorinated phase occurs simultaneously with a decomposition of the fluorinated phase. The average copper oxidation state in this sample was found to be equal to +1.96. Taking into account that the copper-containing admix-

(11) Francesconi, M. G.; Slater, P. R.; Hodges, J. P.; Greaves, C.; Edwards, P. P.; Al-Mamouri, M.; Slaski, M. *J. Solid State Chem.* **1998**, *135*, 17.
(12) Pederzolli, D. R.; Attfield, J. P. *J. Solid State Chem.* **1998**, *136*, 137.
(13) Choisnet, J.; Mouron, P.; Crespin, M.; van Aken, P. A.; Müller, W. F. *J. Mater. Chem.* **1994**, *4*, 895.

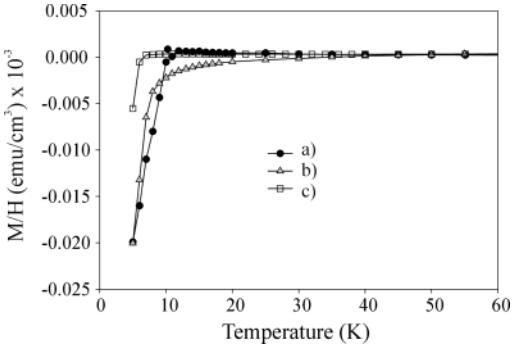

Figure 2. Temperature dependence of the volume magnetic susceptibility for the samples fluorinated at (a) 200 °C with $Nd_2CuO_{3.5}/XeF_2 = 1{:}1.3$, $T_c = 11$ K; (b) 300 °C with $Nd_2CuO_{3.5}/XeF_2 = 1{:}1$, $T_c = 8$ K; and (c) 300 °C with $Nd_2CuO_{3.5}/XeF_2 = 1{:}1.3$, $T_c = 6$ K.

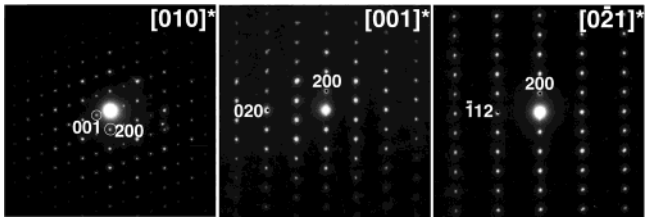

Figure 3. Single domain ED patterns of $Nd_2CuO_{3.5}$. Indexation is made in the monoclinic supercell.

ture was found to be CuO only, we can evaluate the Cu valence in the fluorinated T′ phase as close to +2. Variation of the fluorination temperature in the range 200−400 °C and the molar $Nd_2CuO_{3.5}/XeF_2$ ratio in the range 1−1.3 does not affect the phase compositions of the samples, except for an increasing amount of decomposition products at 400 °C.

Zero field cooled DC susceptibility measurements of samples fluorinated at 200−300 °C exhibit drops associated with a diamagnetic shielding at $T \approx 6-11$ K (Figure 2). The superconducting transition temperature, T_C, is taken as the onset of diamagnetism.

As was found earlier for numerous fluorinated cuprates, soft fluorination at low temperatures (200−400 °C) with various fluorinating agents including XeF_2 can be considered as a nonequilibrium process. An equilibrium interaction of a complex cuprate with XeF_2 results in decomposition with a formation of fluorides and oxyfluorides of alkali-earth and rare-earth elements, which have large lattice energies and hence are thermodynamically very stable. In most cases, the low temperature nonequilibrium fluorination leads to products with a high concentration of defects, which strongly affects X-ray powder pattern and in turn makes structure refinement impractical. The X-ray diffraction pattern of the fluorinated phase in Figure 1 exhibits broadening and a strong asymmetry at the low-angle side of the reflections with indices $l \neq 0$. This feature may indicate local variations of the *c* parameter of the tetragonal cell. Because of this peculiarity we applied transmission electron microscopy for the structural characterization of the fluorinated T′-type phase, and the initial $Nd_2CuO_{3.5}$ material as well, because no electron microscopy study of this compound has been performed previously.

2. Electron Microscopy Study. *2.1. $Nd_2CuO_{3.5}$.* Single domain ED patterns of $Nd_2CuO_{3.5}$ are shown in Figure 3. All ED patterns were completely indexed on the basis of a monoclinic unit cell with the parameters determined from X-ray diffraction data. The only extinction condition observed, *hkl*: $h + k = 2n$, matches with the *C*2/*m* space symmetry. The relationship between the basic vectors of the tetragonal Nd_2CuO_4 unit cell and the monoclinic supercell is given by the following matrix:

$$\begin{pmatrix} -1 & 0 & 1 \\ 0 & 1 & 0 \\ 2 & 0 & 0 \end{pmatrix}$$

According to the crystal structure of $Nd_2CuO_{3.5}$,[12] the superstructure is caused by the ordering of the anion vacancies and oxygen atoms in the ($CuO_{1.5}\square_{0.5}$) planes with the appearance of $h/2,0,l/2_T$ ($_T$ stands for the tetragonal Nd_2CuO_4 subcell) reflections as can be seen on the $[010]^* = [010]_T^*$ pattern. When viewed along *b*, the ($CuO_{1.5}\square_{0.5}$) layers are imaged as projections of (CuO), (O), and ($Cu_\square$) chains alternating along the *c* axis. The separate projections of the (CuO) and the ($Cu_\square$) columns allow the superstructure to be observed along the $[010]^* = [010]_T^*$ direction.

A topotactic oxygen removal from Nd_2CuO_4 results in a reduction of point and translation symmetries according to the following symmetry tree (the transformation of unit cell vectors is shown in brackets): *I* 4/*m* 2/*m* 2/*m* (**a**, **b**, **c**) → *I* 2/*m* 2/*m* 2/*m* (**a**, **b**, **c**) → *I* 1 2/*m* 1 (**a**, **b**, **c**) → *C* 1 2/*m* 1 (**a′** = −**a** + **c**, **b′** = **b**, **c′** = 2**a**). A specific feature of the reduced compound is the presence of numerous twins. The mirror planes, lost during the symmetry reduction, become potential interface planes of orientation domains. This is, for example, observed in some of the [010]* ED patterns exhibiting (*h*0*l*, $h = 2n + 1$) superlattice reflections, which are caused by a twin with a $(100) = (001)_T$ twin plane. (Figure 4). Such a reflection twin results in an interchange of the 002 and $\bar{2}02$; reciprocal lattice vectors. In this case the loss of the mirror plane *m* originally perpendicular to the 4-fold axis results in a twin interface plane lying at the ($CuO_{1.5}\square_{0.5}$) plane (Figure 4). On the ED patterns in Figure 5, taken from other types of twinned regions, the row of reflections

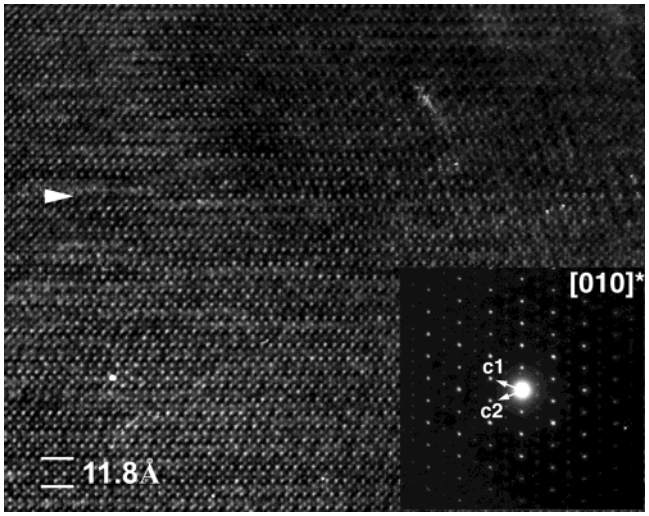

Figure 4. [010] HREM image of a (100) mirror twin in $Nd_2CuO_{3.5}$. The interface is marked by an arrowhead. The corresponding diffraction pattern is shown as an inset.

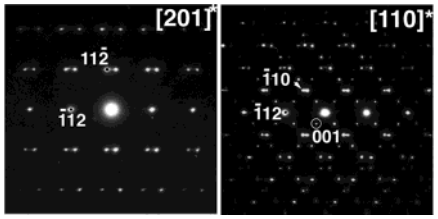

Figure 5. ED patterns taken from regions containing ($\bar{1}12$) mirror twins. The reflections along the [$\bar{1}12$]* row are unsplit.

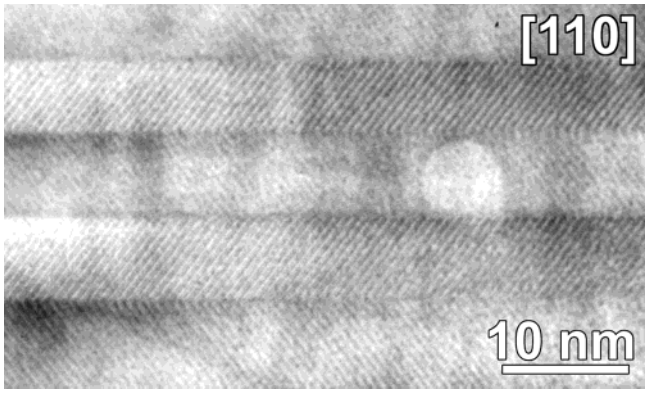

Figure 6. Low magnification [110] image of ($\bar{1}12$) mirror twins.

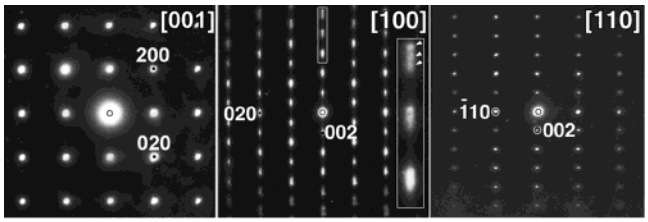

Figure 7. ED patterns of the T′-type fluorinated phase (200 °C, $Nd_2CuO_{3.5}/XeF_2$ = 1:1.3). Note the splitting of the reflections with large *l* indexes on the [100] pattern and on the inserted enlargement.

along [$\bar{1}12$]* is unsplit, whereas all other reflections are split and the direction of splitting is parallel to an unsplit row. This indicates mirror twins with a ($\bar{1}12$) = $(110)_T$ twin plane. A low magnification multibeam image along the [110] direction corresponding to the bottom diffraction pattern in Figure 5 is shown in Figure 6.

2.2. Fluorinated Phases. The electron diffraction patterns of the sample fluorinated at 200 °C with $Nd_2CuO_{3.5}/XeF_2$ = 1:1.3 show the presence of the main phase with a body-centered tetragonal unit cell (Figure 7) with $c_T \approx 12.2$ Å. However, ED patterns were occasionally found with the even larger $c_T \approx 12.7$ and 13.1 Å. The analysis of a large number of ED patterns reveals that the variation in the c_T parameter for the phases in this sample occurs in a discrete manner and c_T values are distributed among three regions: $c_T \approx 12.2-12.4$ Å, $c_T \approx 12.6-12.7$ Å, and $c_T \approx 13.1-13.3$ Å. The presence of these three discrete phases is evident from the inserted enlargement of the 00*l* row on the [100]* ED pattern (Figure 7): the reflections are elongated along c_T* and a splitting into three separate spots at large *l* values is observed.

The areas with different c_T parameters exhibit a laminar appearance as shown on the low magnification [100] image (Figure 8). The areas with $c_T > 13$ Å are typically present as narrow bands of one or two unit

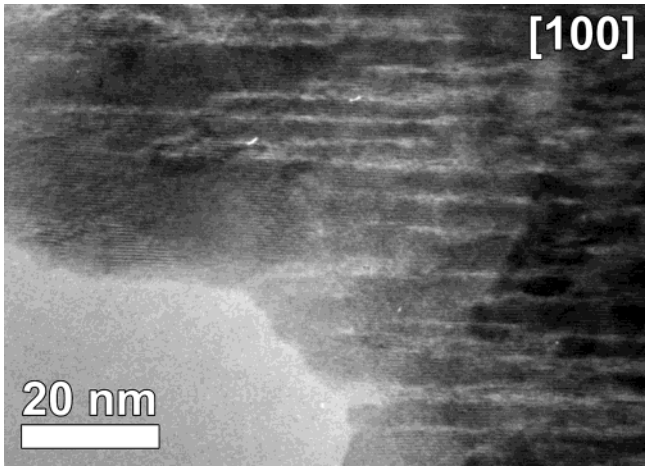

Figure 8. Low magnification [100] image, corresponding to ED patterns in Figure 7. The areas with different c_T parameters appear as alternating bright and dark bands.

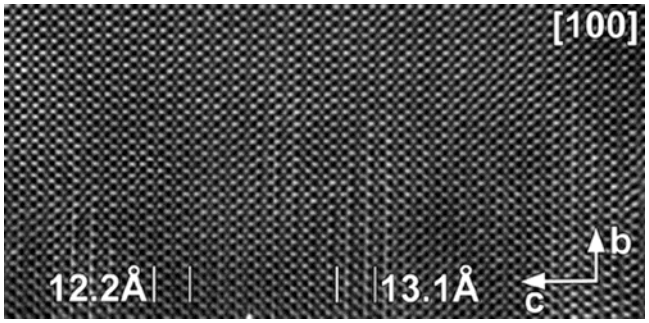

Figure 9. [100] HREM image showing the presence of bands with different c_T parameters.

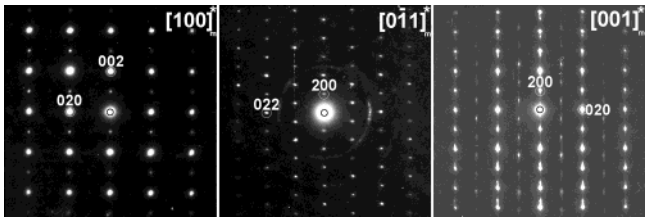

Figure 10. ED patterns of the monoclinic $Nd_2Cu(O,F)_{5-\delta}$ phase (300 °C, $Nd_2CuO_{3.5}/XeF_2$ = 1:1.3). Indexation is made in the monoclinic unit cell.

cells wide in a matrix of the phase with $c_T \approx 12.2$ Å (Figure 9). The HREM images of this main phase exhibit a contrast similar to that observed for the T′ structure. Inclusions of narrow domains with a c_T parameter larger than the c_T of the matrix cause the asymmetric broadening of the $l \neq 0$ reflections in the X-ray powder pattern of this sample.

The fluorination of $Nd_2CuO_{3.5}$ at 300 °C with $Nd_2CuO_{3.5}/XeF_2$ = 1:1 and 1:1.3 has led to the formation of two fluorinated phases (as well as the decomposition products NdF_3 and CuO). The first one corresponds to the fluorinated tetragonal T′-type phase already observed in the sample fluorinated at 200 °C, whereas the ED patterns of the second phase (Figure 10) show a close resemblance to the ED patterns described recently for the monoclinic $Nd_2Cu(O,F)_{5-\delta}$ compound prepared by a fluorination of Nd_2CuO_4.[14] These patterns were

(14) Hadermann, J.; Van Tendeloo, G.; Abakumov, A. M.; Rozova, M. G.; Antipov, E. V. *J. Solid State Chem.* **2001**, *157*, 56.

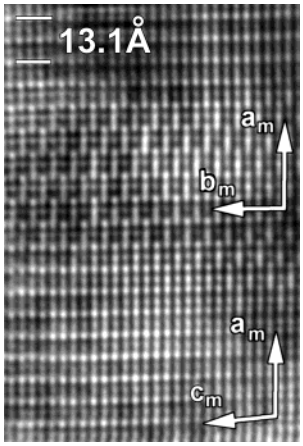

Figure 11. HREM image of a twinned region of the $Nd_2Cu(O,F)_{5-\delta}$ phase. The $[001]_M$ and $[010]_M$-oriented domains are shown.

indexed by a monoclinic unit cell with parameters $a_M \approx 13.2$ Å, $b_M \approx 5.5$ Å, $c_M \approx 5.8$ Å, $\beta \approx 92°$, and space group $C2/c$. The tetragonal and monoclinic fluorinated phases coexist in the same crystallites, but in the sample treated at 300 °C with $Nd_2CuO_{3.5}/XeF_2 = 1:1$ the monoclinic phase often forms separate crystallites. The HREM image of the monoclinic phase exhibits twins with the alternation of $[001]_M$ and $[010]_M$ oriented domains along a_M (Figure 11). This twinning and the image contrast observed in both types of domains are identical to those recently found for the $Nd_2Cu(O,F)_{5-\delta}$ structure.[14] As a consequence, we assume that the monoclinic phase, present in the samples of $Nd_2CuO_{3.5}$ fluorinated at 300 °C, adopts the same structure as that proposed for $Nd_2Cu(O,F)_{5-\delta}$. Structural correlations between these fluorinated phases will be discussed more extensively below. It should be noted that the $(100)_M = (001)_T$ planes in this phase have a wavy shape because of local changes in the c_T parameter.

Attempts to show a presence of fluorine in these materials using EDX analysis were hampered by the low energy of the fluorine K emissions and the overlapping of the F K_α and Nd $M\varsigma$ peaks. Nevertheless, a comparison of the EDX spectra taken from the initial $Nd_2CuO_{3.5}$ phase, and from the monoclinic $Nd_2Cu(O,F)_{5-\delta}$ (Figure 12) reveals that the monoclinic $Nd_2Cu(O,F)_{5-\delta}$ shows a distinct difference between the intensity ratios of the O K_α and the (F K_α + Nd $M\varsigma$) peaks that gives an indirect demonstration of the partial replacement of oxygen by fluorine in the $Nd_2Cu(O,F)_{5-\delta}$ phase.

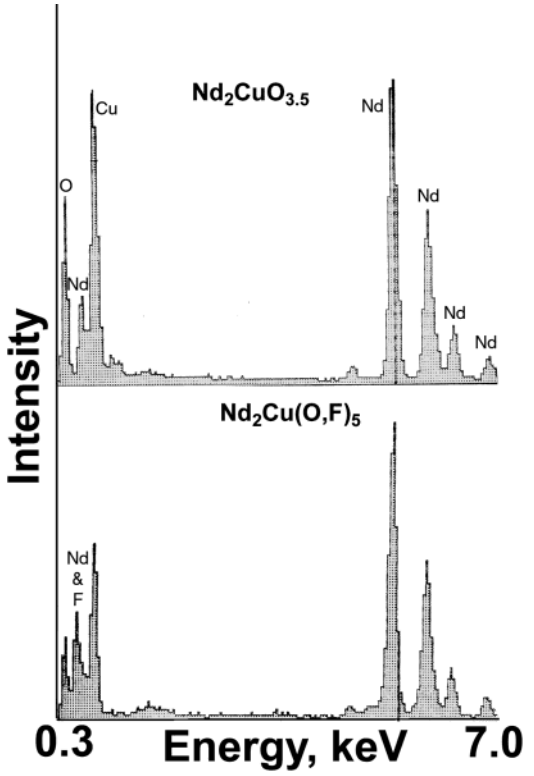

Figure 12. EDX spectra of the initial $Nd_2CuO_{3.5}$ and of the monoclinic $Nd_2Cu(O,F)_{5-\delta}$ phases.

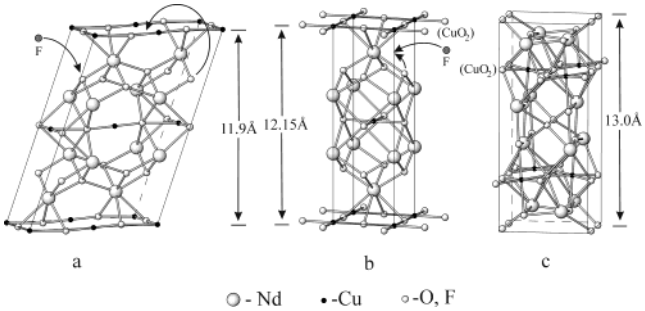

Figure 13. Scheme of the structure transformations under fluorination of $Nd_2CuO_{3.5}$. Structure of (a) the reduced compound $Nd_2CuO_{3.5}$ with a linear coordination for copper; (b) main fluorinated phase with a CuO_4 squares and a T′ structure, fluorine occupies the tetrahedral positions in the fluorite type $Nd_2(O,F)_2$ block; and c) highly fluorinated $Nd_2Cu(O,F)_{5-\delta}$ phase with oxygen and fluorine distributed over both the octahedral and tetrahedral positions of the $Nd_2(O,F)_3$ blocks, forming chains.

Discussion

The structural observations, made with the help of ED and HREM, shed light on the possible sequence of the structure transformations occurring due to the fluorination of $Nd_2CuO_{3.5}$. The insulating $Nd_2CuO_{3.5}$ phase, containing Cu^+, is built up from an alternate stacking of $(CuO_{1.5}\square_{0.5})$ planes and fluorite-type Nd_2O_2 layers.[12] After fluorination at 200 °C, an increase of the formal copper valence (by iodometric titration) and the occurrence of superconductivity (by magnetic measurements) are noted, which imply the formation of (CuO_2) planes. These observations are in agreement with the X-ray diffraction and electron microscopy study which have shown that the main fluorinated phase adopts a tetragonal T′-type structure. It is reasonable to suppose that the fluorination occurs in the fluorite-type Nd_2O_2 blocks, replacing oxygen in the tetrahedral interstices followed by a migration of the oxygen atoms into the vacant anion sites located in the $(CuO_{1.5}\square_{0.5})$ planes (Figure 13). This process has an oxidative character because the oxygen atoms are not removed from the structure. An additional oxidation can occur due to the insertion of extra fluorine atoms into the octahedrally coordinated interstices of the $Nd_2(O,F)_2$ block with the formation of apical bonds with the Cu atoms. Taking into account that the oxidation could also be caused by an oxygen insertion, because oxygen is released by a formation of NdF_3 admixture, we have performed an estimation of partial oxygen pressure inside the Cu tube.

After the fluorination was carried out we have found that a thin layer of Cu_2O covers the inner walls of the copper tube, as it was always observed if the fluorination of complex copper oxide using similar experimental setup is accompanied by a replacement of oxygen by fluorine or partial decomposition.[15] Assuming that oxygen reacts with Cu, forming Cu_2O, one can estimate the equilibrium partial oxygen pressure at 500 K as lg($P(O_2/atm)$) = −28.2, according to the data from reference 16. The equilibrium partial oxygen pressure of the reduction of Nd_2CuO_4 to the Cu^+-containing phase $NdCuO_2$ by the reaction $2Nd_2CuO_4 = 2NdCuO_2 + Nd_2O_3 + {}^1/_2O_2$ was found to be much higher (lg($P(O_2/atm)$) = −21.8, calculated using the data from Petrov et al.[17] extrapolated to T = 500 K). This comparison indicates that oxygen cannot act as an oxidizer in our experimental setup and fluorine insertion is responsible for increasing the formal copper valence.

Extra anions expand the copper coordination environment to tetragonal pyramids and, ultimately, to octahedra. The Jahn−Teller effect, inherent for Cu^{2+} cations, leads to the elongation of the Cu−F apical bonds and an expansion of the unit cell along the c_T axis. The bands with three different c_T areas were found in the fluorinated phase, and three different discrete $c_T/3a_T$ ratios can be calculated from the observed ED patterns: 1.03, 1.07, and 1.11. These values are very close to the typical $c_T/3a_T$ ratios observed for the T′, T*, and T phases of 1.02, 1.07, and 1.15, respectively.[18] We can assume that the discrete values of c_T for the fluorinated tetragonal phase, correspond to regions showing the three types of copper coordination found in T′ (square), T* (square pyramid), and T (octahedron) structures. The main phase is the T′ type which is probably responsible for the superconductivity in the fluorinated samples.

The superconducting properties of fluorinated $Nd_2CuO_{3.5}$ samples can be compared with those of $Nd_2CuO_{4-x}F_x$ solid solutions. The latter were prepared either by a solid-state reaction with subsequent reductive treatment using NdF_3 as a source of fluorine[7,19,20] or by a low-temperature fluorination of Nd_2CuO_4 by NH_4F,[21] and exhibit the homogeneity range up to $x \approx 0.3$.[19] The maximal temperature of the superconducting transition for $Nd_2CuO_{4-x}F_x$ materials (T_C = 27 K, $0.2 \le x \le 0.3$)[7,8] is significantly higher than that observed for fluorinated $Nd_2CuO_{3.5}$ samples (T_c = 6−11 K). This difference can be related to either not optimal copper oxidation state or to a partial occupation of anion positions in conducting layers by fluorine. Superconductivity has been observed in fluorinated T′ phase of n-type only,[22] and the same type of carrier is assumed to be present in the superconducting fluorinated samples investigated here. Indeed, the average Cu valence of +1.96, as it was found for the sample fluorinated at 200 °C with $Nd_2CuO_{3.5}/XeF_2$ = 1:1.3, is too high for n-type superconductivity in the T′ phase, where the optimally doped state is achieved near V_{Cu} = +1.85, but high copper valence can be explained by the presence of a small amount of CuO in the sample. On the other hand, partial replacement of oxygen by fluorine in conducting (CuO_2) layers also takes place in $Nd_2CuO_{4-x}F_x$ samples where above 30% of fluorine was found in the (CuO_2) layers for x = 0.15 and 0.3 by XAFS study.[23] From this point of view it is difficult to conclude without a doubt what is responsible for lowering T_c in fluorinated $Nd_2CuO_{3.5}$ samples in comparison with that in $Nd_2CuO_{4-x}F_x$ solid solutions.

The mechanism of anion rearrangement resulting in a transformation of monoclinic $Nd_2CuO_{3.5}$ into tetragonal T′ structure is similar to that observed in fluorinated Sr_2CuO_3.[10] Calculations of the electrostatic energies for different oxygen and fluorine distributions between the rocksalt blocks and the Cu layers in that case revealed that the driving force of this rearrangement is a gain in the electrostatic energy when fluorine is located in the rocksalt block and oxygen is located in the Cu layers, creating (CuO_2) layers. We have performed a similar evaluation of the structure stability for anion stoichiometric T′-type $Nd_2CuO_{3.5}F_{0.5}$. Two possibilities were considered: (1) all tetrahedral interstices in the fluorite slab are occupied by oxygen and the fluorine atoms are located at the ($CuO_{1.5}F_{0.5}$) layers; or (2) (CuO_2) layers are formed in the structure and the composition of the fluorite slab is $Nd_2O_{1.5}F_{0.5}$. For both cases the Madelung constant computations were made using the Ewald method.[24] The atomic coordinates were taken from the Nd_2CuO_4 structure, and the charges were calculated as a weighted average of the formal charges, where the occupancy factors were taken as the weight factors. The calculation showed that the structure (2) has a lower energy than (1) by ∼200 kJ/mol, and the replacement of oxygen atoms for fluorine with the subsequent migration of oxygen into the ($CuO_{1.5}\square_{0.5}$) layers is thus most probably driven by a gain of electrostatic energy.

At 200 °C the fluorination may preferentially occur as a fluorine insertion. At 300 °C a further fluorination involving anion exchange takes place. The replacement of one oxygen by between one and two fluorine atoms induces an increase of the fluorine content, as was shown by the EDX spectrum of the fluorinated monoclinic $Nd_2Cu(O,F)_5$ phase. When both tetrahedral and octahedral interstices in the $Nd_2(O,F)_{2+x}$ block are occupied by a significant amount of anions, the anion−anion distances become close to 2−2.15 Å and strong repulsive forces lead to a structure transformation from the tetragonal to the monoclinic $Nd_2Cu(O,F)_5$ phase. The structural model of this phase (Figure 13c) was recently deduced from an EM investigation of fluorinated Nd_2CuO_4.[14] It involves an ordered occupation of the anion sites between two adjacent Nd layers by anions and anion vacancies and the partial migration of the anions from these tetrahedrally coordinated positions to the octahedral interstices forming the apical vertexes of the

(15) Abakumov, A. M.; Rozova, M. G.; Ardashnikova, E. I.; Antipov, E. V. *Russ. Chem. Reviews* **2002**, *71*, 383.
(16) IVTANTHERMO, Database of thermodynamic properties of individual substances, THERMOCENTER, Russian Academy of Sciences: Moscow, 1993.
(17) Petrov, A. N.; Cherepanov, V. A.; Zuyev, A. Yu.; Zhukovsky, V. M. *J. Solid State Chem.* **1988**, *77*, 1.
(18) Abakumov, A. M.; Antipov, E. V.; Kovba, L. M.; Kopnin, E. M.; Putilin, S. N.; Shpanchenko, R. V. *Russ. Chem. Rev.* **1995**, *64*, 719.
(19) Sugiyama, J.; Ojima, Y.; Takata, T.; Sakuyama, K.; Yamauchi, H. *Physica C* **1991**, *173*, 103.
(20) Lopez-Morales, M. E.; Grant, P. M. *J. Solid State Chem.* **1990**, *85*, 159.
(21) Asaf, U.; Felner, I.; Yaron, U. *Physica C* **1993**, *211*, 45.
(22) Sugiyama, J.; Kosuge, M.; Ojima, Y.; Yamauchi, H.; Tanaka, S. *Physica C* **1991**, *179*, 131.
(23) Krol, A.; Soo, Y. L.; Ming, Z. H.; Huang, S.; Kao, Y. H.; Smith, G. C.; Lee, K.; James, A. C. W. P.; Murphy, D. W. *Phys. Rev. B* **1992**, *46*, 443.
(24) Popov, S. G.; Levitskiy, V. A. *Zh. Fiz. Khim.* **1981**, *LV*, 87 (Russ.).

$Cu(O,F)_6$ octahedra. The chains of filled and vacant tetrahedral positions run along the b_M axis and alternate along c_M. The $Cu(O,F)_6$ octahedra are tilted around b_M to maximize the distances between neighboring anions.

Acknowledgment. This work was financially supported by the Royal Society, IUAP 4/10, and Russian State Program on Superconductivity (Poisk). G.C. thanks the European Commission for a Marie Curie Individual Fellowship. A.M.A. is grateful to the scientific council of Moscow State University for a research fellowship. We also are grateful to G. Van Tendeloo for scientific discussions on the subject and to B. Ph. Pavlyuk for the help in sample preparation.

CM021102M